Indian Journal of Pure & Applied Physics
Vol. 58, March 2020, pp. 168-177

Preferential solvation and bimolecular quenching reactions of boronic acid dye at very low quencher concentrations studied by fluorescence spectrum in toluene and butanol binary mixtures

P Bhavya[a], Raveendra Melavanki[b*], Raviraj Kusanur[c] & J Thipperudrappa[d]

[a]Department of Physics, New Horizon College of Engineering, Bengaluru 560 103, India

[b]Department of Physics, M S Ramaiah Institute of Technology, Bengaluru 560 054,India

[c]Department of Chemistry, R V College of Engineering, Bengaluru 560 059, India

[d]Department of Studies in Physics, Vijayanagara Sri Krishnadevaraya University, Vinayaka Nagara, Ballari 583 105, India

Received 27 September 2018; accepted 26 June 2019

Inferable from the significance of solvent mixtures in practical chemistry, toluene (TL) and butanol (BL) mixtures are used to studyfluorescence behavior of boronic acid dye 2-methoxy-5-fluoro-phenyl boronic acid (2MEFPBA). At the inception, preferential solvation is examined in TL-BL, to understand specific and nonspecific interactions. Suppan's dielectric enrichment model is further used to understand the nonideality and dielectric enrichment in TL-BL mixtures for preferential solvation. Bimolecular quenching reaction studies of 2MEFPBA with aniline as quencher are made in mixtures of TL–BLto know the effect of viscosity and dielectric constant variation at room temperature.

The quenching process is studied in all solvent mixtures by steady state and transient state method. Quenching is characterized by S-V plots having upward curvature. Analysis of modified S-V equations which accounts both static and dynamic quenching allows calculating bimolecular quenching rate constant. The bimolecular quenching reactions are found to be significantly larger. Further finite sink approximation model is invoked so as to check whether reactions are diffusion limited. The extents of these rate parameters demonstrate that positive deviations in the Stern-Volmer (S-V) plot are because of the presence of apparent static and dynamic quenching process.

Keywords: 2 MEFPBA, Preferential solvation index, Suppan's theory, High bimolecular quenching rate constant, Sphere of action, Finite sink approximation model

1 Introduction

It has been long recognized that solvation processes are essential to our understanding of chemical reactions in the liquid phase. Solvent mixtures make a highly appropriate medium, much better than pure solvents with enhanced physical properties like solvation power, viscosity, density, vapor pressure, refractive index, relative permittivity and freezing/boiling point. Understanding of physio-chemical properties becomes complex with regard to solute-solvent interactions in mixed solvents than in pure solvents[1]. Ranging from study of reaction kinetics, chromatographic separations in organic synthesis to hydrometallurgical application, mixed solvents are used normally in practical chemistry[2-6]. In some cases, by nature, liquid mixtures are the default medium obtained as in crude oil, while in other cases, mixture medium helps enhance the physical characteristics of solvent medium such as polarity, density, viscosity etc. for which they are specifically designed and this is used for discrete requirements so as to affect reaction kinetics, yield desirable products and to improve solubility[7]. Binary solvent mixtures provide medium where it is possible to vary the solvent-solvent interaction as such; study in these media is expected to throw more light on understanding the solvation process[8]. Also, the mixed solvent system helps us to clearly understand the role of relative variation in solvent polarity and viscosity of the medium on fluorescence quenching experiments. Thus, our present work reports the effects of binary mixtures on preferential solvation and bimolecular quenching reactions.

Bimolecular quenching reactions of fluorescent molecules in solutions by external quenchers are illustrated by:

$$F^* + [Q] \xrightarrow{k_q} Product$$

---

*Corresponding author (E-mail: melavanki73@gmail.com)

Most of quenching process involves an excited fluorophore molecule interacting F^* with quencher molecule Q where, k_q represents rate constant for the bimolecular process. Various quenchers like aromatic and aliphatic amines, metal ions, halide ions, C_6H_5Br, CCl_4, $C_3H_7KS_3$ and CH_3NO_2 etc. have been used by several investigators to study steady state and transient state effects[9-13]. Investigation of observed bimolecular quenching rate constant provides much information about fluorophore and its environment. Thus, fluorescence quenching plays a sensory role which serves numerous categories of beneficiary including biology, physical science and medical science and in chemical analysis. Investigation of kinetics of photo-physical inter-molecular quenching process and calculation of bimolecular quenching rate constant is through using well known Stern-Volmer equation. In majority, experimental analysis of fluorescence quenching using Stern-Volmer (S-V) relation shows linear dependency which is analyzed as due to pure static or dynamic quenching alone and is given by:

$$\frac{I_0}{I} = 1 + K_{SV}[\mathrm{Q}] \quad \ldots (1)$$

Where, I_0 is the fluorescence intensity of F and I is the fluorescence intensity of $F^* + [Q]$. The Stern-Volmer constant K_{SV} calculated by slope of the plot I_0/IVS, Q is used to calculate bimolecular quenching rate constant k_q by the equation $K_{SV} = k_q\tau_0$. Here, τ_0 represents the lifetime of the fluorophore. But in some cases, it's also been observed that certain quenching reactions show curved S-V plots. Both upward[12-14] and downward curvatures[15-17] have been observed by many researchers, while positive deviation is ascribed to various processes like combined static and dynamic quenching, inter system crossing and formation of charge transfer complexes both at ground and excited states. Negative deviation in S-V plots is analyzed due to heterogeneity of the system, selective quenching, hydrogen bond complex formation and occurrence of reversible photochemical process. To remarkable extent quenching mechanisms are affected by solvent polarity, solvent viscosity and the range of quencher concentration.

Boronic acids and their derivatives which are regarded as green compounds continue to gain interest in the areas of fluorescence imaging, biomedical engineering, chemosensing, chemical biology, mass spectrometry as well as in synthetic, organic, materials and bioorganic chemistry. They show remarkable sensitivity form on osaccharides with high percentage of α and β furanose forms[18]. Their unique properties combined with their stability, simplicity of handling and their reactivity as mild organic lewis acids are what instigated us to take up the studies on boronic acid derivatives. Effect of substitution, solvent viscosity and polarity on boronic acid derivative 2-methoxy-5-fluoro phenyl boronic acid is analyzed through bimolecular quenching reactions. Role of solvent polarity and solvent viscosity on fluorescence quenching and its mechanisms is better understood in solvent mixtures hence quenching analysis is carried out in solvent mixtures of toluene (TL)–butanol (BL) at room temperature. Also critical literature review shows no traces of using mixtures of aprotic solvent TL and protic solvent BL for quenching studies and this is chosen to see any solvent-solvent interaction affecting quenching process. These solvent mixtures provide a good range of viscosity (0.496-1.982 m pa s) and dielectric constant (2.38-17.565) variation. Steady state techniques are used to study fluorescence quenching by aniline as quencher insolvent mixtures. Bimolecular quenching reactions are characterized by various rate parameters which are determined by sphere of action static quenching model and finite sink approximation model.

2 Experimental Details

The boronic acid dye 2-methoxy-5-fluoro phenyl boronic acid is prepared by standard method[19] whose molecular structures are depicted in Fig. 1. Spectroscopic grade solvents toluenen (TL) and butanol (BL)are used without any further purification. Doubly distilled anilineis used as quencher after it is tested for its purity. The solutions were prepared by keeping boronic acid dye concentration fixed at 1×10^{-5}M/L. Quenching is found to be observed at very

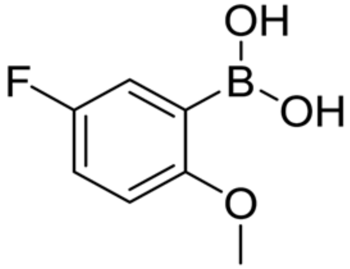

Fig. 1 — Molecular structures of dye.

low quencher concentration, hence quencher concentrations were taken in the range of 0.000–0.005 M in all the TL-BL solvent mixtures. Absorption measurements are made with wavelength accuracy of 0.5 nm in UV-Vis spectrophotometer (model: shimadzu UV-1800) and the excitation wavelength is found to be 285 nm. Hitachi fluorescence spectrophotometer F-2000 with perpendicular geometry is made use for fluorescence measurement. Solutes are excited at their respective excitation wavelength at room temperature by taking fresh solution each time in a rectangular quartz cell having an air tight stopper where slit width (5 nm:5 nm), operating voltage(400 v) are maintained constant throughout the measurements. Aniline used as quencher has absorption maxima at 280 nm which is close to the excitation wavelength of dye which may pose inner filter effect (IFE) which deludes the quenching analysis. This is handled appropriately by applying the proper correction as mentioned in the literature[20] by using the equation:

$$I_{real}/I_{measr} = \left[2.303D\left(d_2 - d_1\right)\right]/\left[10^{-Dd_2} - 10^{-Dd_1}\right]$$

Here, I_{real} and I_{measr} are real and measured emission intensities, d_1 and d_2 are cuvette dimensions and $D = \varepsilon Q$ (ε =molar absorption co-efficient of aniline, Q =aniline concentration). After the necessary IFE corrections typical fluorescence spectrum in 60 % TL and 40 % BL solvent mixtures without aniline and with the said low concentration of aniline is shown in Fig. 2 at a fixed solutes concentration. Fluorescence lifetime τ_0 (without the quencher) and τ (with the quencher) of the solutes was measured by using led as excitation source at excitation wavelength 285 nm for dye, respectively. In photophysics model of TCSPC nanosecond fluorescence spectrometer available at USIC Dharwad, Karnataka, India. The fluorescence decay profiles of both boronic acids dye recorded in 60 % toluene and 40 % butanol solvent mixtures with the quencher concentration of 0.000 M is shown in Fig. 3. The experimental values are reproducible within 5 % of the experimental error.

3 Results and Discussion

3.1 Preferential solvation dynamics studies in TL-BL mixtures

In binary solvent mixture, dissolved polar solute responds differently with individual solvent components. Hence, one can reasonably presume that the micro environment within solvation sphere of the solute has a different composition from the bulk counter part. Due to this, properties of solute will deviate from a direct dependence on solvent composition which has been qualitatively rationalized by using the concept of preferential solvation by many research groups[21]. Preferential solvation is the consequence of either dielectric enrich mentor through specific solute-solvent interactions. When solvent molecules lie closer to the solute molecule, specific exchanges like inter-molecular hydrogen bonds get established between solute-solvent molecules. Typically, these are strong interactions between the single solute and a single solvent molecule and are directional. Dielectric enrichment on the other hand, is due to polar solvent molecules

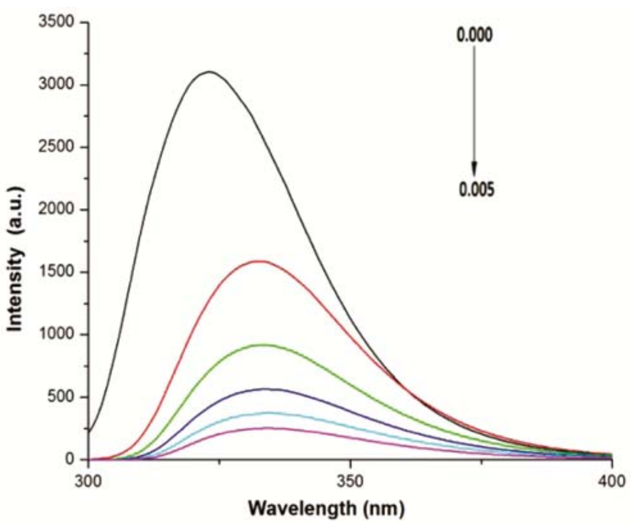

Fig. 2 — Emission spectra of boronic acid dye in 60 % TL + 40 % BL with varying quencher concentrations 0.00, 0.001, 0.002, 0.003, 0.004 and 0.005 M.

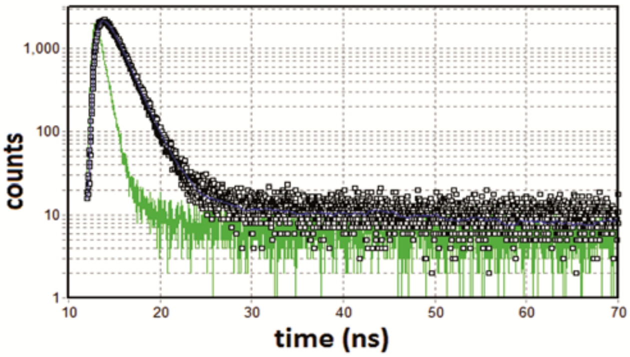

Fig. 3 — The fluorescence decay profile of boronic acid dye in 60 % TL + 40 % BL with varying quencher concentration of 0.00M.

getting attracted to solute charge distribution, which gets manifested as centralization of the polar solvent element throughout the solvation sphere adjacent to solute. This solvation sphere enrichment to a good approximation has spherical symmetry which is analyzed under the assumption of a continuum solvent shell model[22]. While studying preferential solvation, one should be responsive to realize that functional groups that participate in specific interactions often have very large dipole moments due to which specific and non-specific interaction mechanisms, although different, may often occur in tandem[23]. To understand specific solute-solvent and solvent-solvent interactions through preferential solvation of the 2MEFPBA, studies have been carried out in binary solvent mixtures.

Two different methods are employed to calculate the magnitude of preferential solvation. In the first case[24], preferential solvation is expressed by the 'local' excess or deficiency of one solvent component over the bulk composition, i.e.,

$$X_2^L = \frac{\vartheta_{12}-\vartheta_1}{\vartheta_2-\vartheta_1} \qquad \ldots (2)$$

Where, ϑ_1,$\vartheta_2$and ϑ_{12} are the values of the electronic transition energy in the solvents 1 and 2, respectively. X_1 and X_2 are the bulk mole fractions of the solvents 1 and 2 while $X_1^L$and X_2^L are the mole fraction in the cybotactic region. Index of preferential solvation with respect to co-solvent is then calculated by:

$$\delta_{s2} = X_2^L - X_2 \qquad \ldots (3)$$

The second method[25] incorporates proportionality coefficient of the ratio of the molecules of solvent 2 in reference to solvent 1 in the cybotactic region of the solute given by parameter f_2/f_1. It is the ratio of molecules of the same solvent in reference to the other in the bulk of the solution, where:

$$\frac{f_2}{f_1} = \left(\frac{X_1}{X_2}\right)\left(\frac{\vartheta_{12}-\vartheta_1}{\vartheta_2-\vartheta_{12}}\right) \qquad \ldots (4)$$

This parameter is equivalent to the exchange constant[26] K_{ps} for the description of E_T (30) variation with composition in binary mixtures, where

$$K_{ps} = \frac{X_2^L X_1}{X_1^L X_2}.$$

Figure 4 shows the variation of ν_{12} with increasing BL mole fraction for both absorption and emission maxima's in 2 MEFPBA. In these plots clear deviation from the ideal linearity allows to predict preferential solvation of solute without any observed synergism. The outcomes of the experimental data in the mixtures are tabulated in Table 1 for absorption and emission maxima's of 2 MEFPBA. A critical analysis of the tabulated data reveals that increasing BL concentration reduces ν_{12}. We see δ_{s2} is negative and $\frac{f_2}{f_1} < 1$ suggesting the compound is solvated by TL in its ground state. In excited state of the dye, +ve and $\frac{f_2}{f_1} > 1$ for all mole fractions of BL clearly indicates that dye are preferentially solvated by more polar solvent BL.

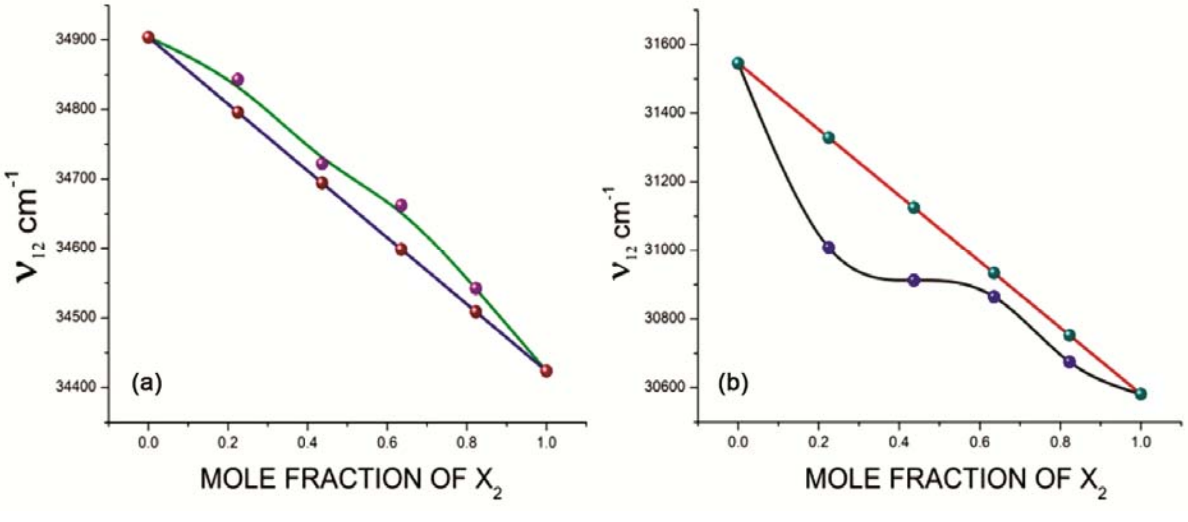

Fig. 4 — Plot of ν_{12} versus mole fraction of BL(X_2) in TL+BL mixture (a) absorption and (b) emission of dye.

To understand preferential solvation with non-specific interactions in the studied solvent mixture systems through dielectric enrichment, Suppan's theory of single shell approximation for dielectric enrichment is applied. According to this, deviation from non-linearity in absorption and emission maxima also may arise mainly due to non-ideal behavior of solvent mixtures in terms of dielectric constant (ε) dependency on solvent mole fractions. They suggested a continuum reaction field, $\mathrm{F}(\varepsilon) = 2(\varepsilon - 1)/2\varepsilon + 1$ based on experimentally measured ε which provides a much better description. Extent of preferential solvation is represented by preferential solvation index Z_{ps}. Suppan correlated the preferential solvation index (Z_{PS}) with an experimental nonlinearity ratio (ρ_{exp}),which was obtained from the spectral shifts by using Eqs 27 and 28:

$$\rho_{exp} = \frac{2\int_0^1 (\gamma_{exp}-\gamma_{lin,bulk})dx_p}{\Delta\gamma_{p-n}} \qquad \dots (5)$$

Where, γ_{exp} is the absorption or emission-peak energy for a binary mixture with a polar mole fraction of x_p and $\gamma_{lin,bulk}$ is same as for an ideal solvent mixture given by $\gamma_{lin,bulk} = x_p\gamma_p + x_n\gamma_n$. $\Delta\gamma_{p-n}$ represents the stokes shift between the polar and non-polar solvents. Non-ideality in a solvent mixture (ρ_{exp}) arises from both preferential solvation (ρ_{ps}) as well as dielectric non-ideality (ρ_{dn}) [29-30]. ρ_{dn} is calculated by a similar equation as ρ_{exp} given by Eq. (5) with the terms ρ_{exp} and γ replaced with ρ_{dn} *and* Onsager's polarity parameters, respectively and ρ_{ps} is given by $\rho_{ps} = \rho_{exp} - \rho_{dn}$.

Kauffmanand co-workers[30] have shown that there can be a well approximated relation between ρ_{ps} and Z_{ps} given by $\rho_{ps} = 0.31 Z_{ps}$ when ρ_{ps} is less than 1. Above equations provide an independent method of calculating Z_{ps} from experimental spectroscopic data. Figure 5 shows the deviation of TL-BL binary mixtures from their ideal behavior with respect to variation of onsager polarity function of the mixture to polar solvent mole fraction. Deviation in the graph from linearity in the mixtures in the absence of the solute clearly predicts mixture to be non-ideal. The non-linearity ratio calculated from Eq. (5) using onsager polarity function is observed to be ρ_{dn}=0.224. Using Eq. (5) the non-linearity ratios for the dye is obtained where ρ_{exp}= -0.143 for absorption band and for emission band ρ_{exp}=0.292 is observed. Non-linearity ratio ρ_{exp} calculated in its excited state

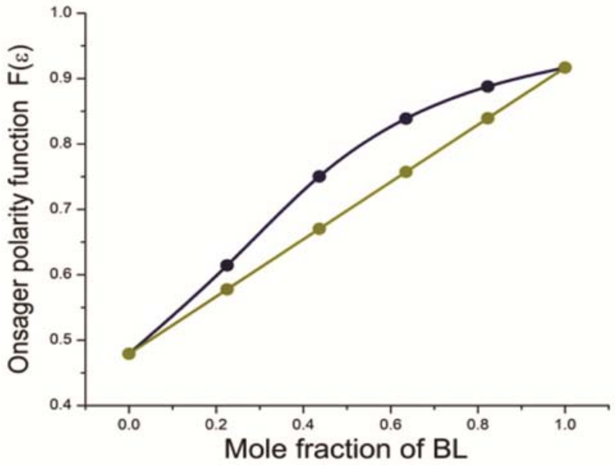

Fig. 5 — Plot of onsager polarity function versus mole fraction of polar solvent X_2in TL + BLmixture.

Table 1 — Values ν_{12} cm^{-1}, bulk mole fraction (X_2) of BL in TL, local mole fractions ($X_1^L$of TL, X_2^L of AN), preferential solvation index δ_{s2} and preferential solvation constant ($\frac{f_2}{f_1}$) for absorption maxima of dye.

Solute		Absorption					Emission				
Mixture ratio	X_2	ν_{12} cm^{-1}	X_1^L	X_2^L	δ_{s2}	$\frac{f_2}{f_1}$	ν_{12} cm^{-1}	X_1^L	X_2^L	δ_{s2}	$\frac{f_2}{f_1}$
TL 100	0.0000	34904	--	--	--	--	31546	--	--	--	--
TL80/ BL 20	0.2250	34843	0.8735	0.1265	-0.0985	0.4989	31008	0.4423	0.5577	0.3327	4.3425
TL60/ BL 40	0.4364	34722	0.6217	0.3783	-0.0581	0.7858	30912	0.3430	0.6570	0.2207	2.4744
TL 40/ BL60	0.6353	34662	0.4965	0.5035	-0.1318	0.5821	30864	0.2935	0.7065	0.0712	1.3817
TL20/ BL80	0.8228	34542	0.2474	0.7526	-0.0702	0.6551	30675	0.0972	0.9028	0.0800	1.9994
BL 100	1.0000	34423	--	--	--	--	30581	--	--	--	--

is clearly greater than that intrinsically created by TL-BL solvent mixtureswhen solute dipole is not present. This indicates that preferential solvation of the solute is through dielectric enrichment by more polar solvent BL is in role rather than specific interaction like hydrogen bonding ability of the alcohol in its excited state. Preferential solvation is not through dielectric enrichment in the case of ground state. These are by ZPS values given by -1.183 and 0.219 excited state.

3.2 Bimolecular quenching reaction studies in TL-BL mixtures

Non-linear Stern-Volmer plots are obtained from fluorescence titration data for dye in all the solvent mixtures. Using experimentally measured values of I_0 and I, upward curvature obtained in both the dyes for all composition of solvent mixtures are shown in Fig. 6. Analysis of similar experimental results observed by others[31-34] suggests that bimolecular quenching reaction is not purely collisional and reveals the role of associated static quenching process. Static quenching implies either formation of ground state complex or existence of effective sphere of action for quenching.

3.2.1 Static and dynamic quenching analysis

3.2.1.1 Ground state complex formation

Possibility of static quenching through ground state complex formation is evaluated using extended S-V equations given by:

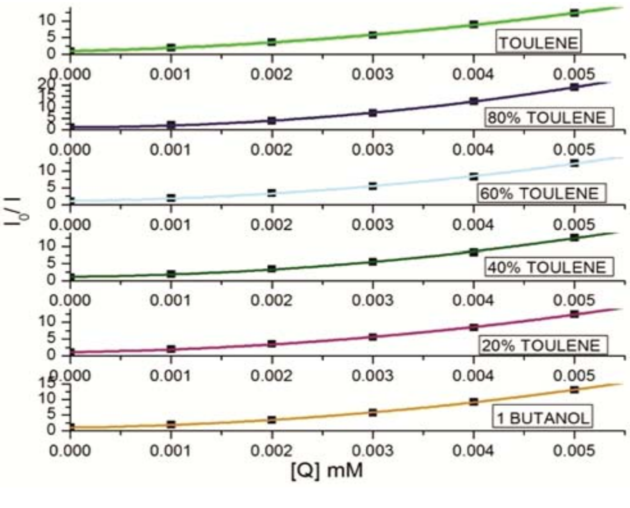

Fig. 6 — Stern-Volmer (S-V) plots from steady state fluorescence emission intensity measurement for boronic acid dye + aniline system in different mixtures of toluene (TL) + 1-butanol (BL) solvents: (i) 100 % TL + 0 % BL (ii) 80 % TL+ 20 % BL (iii) 60 % TL + 40 % BL (iv) 40 % TL + 60 % BL (v) 20 % TL + 80 % BL and vi) 0 % TL + 100 % BL.

$$[(I_0/I)-1]/Q = (K_{SV}+K_g)+K_{SV}K_g[Q] \quad \dots (6)$$

Here, Q and K_{SV} have their previously mentioned meaning and K_g is the ground state association constant. A linear variation is obtained for plot of $[(I_0/I)-1]/Q$ vs Q by least square fit method, from which $K_{SV}K_g$ and $(K_{SV}+K_g)$ are obtained by slope and intercept, respectively. Formation of ground-state complex is confirmed if K_{SV} obtained from Eq. (6) is in agreement with K_{SV} obtained from linear part of the plot at lower concentration region from Eq. (1). In present study K_{SV} obtained from Eq. (6) is imaginary involving complex number. This indicates that there is no ground-state complex formation. Further unaltered absorption and fluorescence spectra at all concentrations of quenchers in all mixture ratios except to the intensity reduction due to quencher addition ascertain non formation of ground-state complex.

3.2.1.2 Apparent static quenching model

In systems even when there is no stable ground-state complex formation substantial upward curvature is accounted by sphere of action static quenching model along with the dynamic quenching. It is assumed that the probability of quenching of the molecule at time of excitation with the quencher is unity inside sphere of volume $\frac{V}{N_A} = (4/3)\pi r^3$ and zero outside it. Here we consider $P_0 = e^{-V[Q]}$ is the probability that no quencher molecule is within the sphere at the time of excitation in which sphere volume V/N_A is the volume actually available to the point-center of the quencher molecule. Since, emission intensity is proportional[34-36] to P_0 S-V equation leads to:

$$\frac{I_0}{I} = 1 + K_{SV}[Q]e^{V[Q]} \quad \dots (7)$$

If we assign

$$W = e^{-V[Q]} \quad \dots (8)$$

as fraction of solute which is quenched by dynamic mechanism then we have $1-W$ are the fraction which are deactivated instantly at the time of excitation by sphere of effective quenching model. Then we have:

$$\frac{I_0}{I} = \frac{1+K_{SV}[Q]}{W} \qquad \dots (9)$$

The above equation can be re-written for fraction of solute quenched due effective sphere as:

$$[1-(I/I_O)]/[Q] = K_{SV}(I/I_O)+(1-W)/[Q] \qquad \dots (10)$$

Above equation is plotted where a straight line is obtained for $[1-(I/I_O)]/[Q]$ against I/I_O and is shown in Fig. 7 for 2 MEFPBA for all solvent mixtures of TL-BL. Plots of Eq. (10) are used to calculate Stern-Volmer quenching constant K_{SV} and $(1-W)/[Q]$ from their slope and intercept, respectively. Using measured values of τ_0 bimolecular quenching rate parameter k_q was determined from relation $k_q = K_{SV}/\tau_0$. To support apparent static quenching model analysis, using the values of W and Eq. (9), magnitudes of static quenching constant V and radii r of sphere of action are determined. Values are tabulated in Table 2 for the dye.

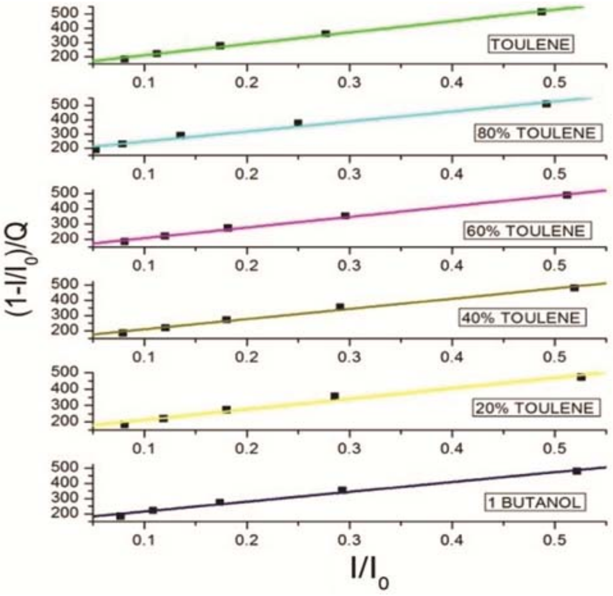

Fig. 7 — Plots of [1-(I/I_0)]/[Q] against I/I_0 for boronic acid dye aniline system in different mixtures of toluene (TL) + 1butanol (BL) solvents:(i) 100% TL + 0% BL (ii) 80 % TL+ 20 % BL (iii) 60 % TL + 40 % BL (iv) 40 % TL + 60 % BL (v) 20 % TL + 80 % BL and vi) 0 % TL + 100 % BL.

The solute radii R_s and the quencher radii R_q molecules were determined as suggested by Edward[37] and are given at the bottom of Table 2. Encounter distance R is determined by the sum of the solute and quencher molecular radii. From Table 2, it is seen that $r > R$ in Dye. Therefore, the conclusions can be drawn according to Andre *et al.*[38] and Zeng *et al.*[39] that static effect is in role whether or not there is formation of stable ground-state complex provided the reactions are limited by diffusion indicating the sphere of effective quenching model fitting well.

Diffusion limited reactions are further ascertained by invoking finite sink approximation model for steady state.

3.2.1.3 Finite sink approximation model

Finite sink approximation model provides the well-known expression[37-40]:

$$1/k_q = (1/k_d)+(1/k_a) \qquad \dots (11)$$

Where, $k_d = 4\pi N'RD$ and k_a is the activation energy controlled rate constant describing the reaction of encountered pairs at a reactive distance *R. D* is the sum of the diffusion coefficients of solute and quencher molecules. Following Eq. (11), k_q is independent of [*Q*]. But for efficient quenching process in liquids, k_q is often observed to increase

Table 2 — The average fluorescence life time (τ_0), S-V constant (K_{sv}), range of W, static quenching constant (V), kinetic distance (r) and quenching rate parameter (k_q) calculated from sphere of action for in different solvent mixtures of toluene (TL) + 1butanol (BL) of boronic acid dye at room temperature.

Solvent mixture		Dielectric constant (ε)	Viscosity(η)	τ_0 (ns)	K_{SV} (M^{-1})	W	V ($mol^{-1}\,dm^3$)	r (A^0)	$k_q \times 10^{-9}$ ($M^{-1}s^{-1}$)
TL	BL								
100	0	2.38	0.496	1.11	797.45	0.869-0.347	227.3	44.84	718.42
80	20	3.39	0.534	1.32	699.4	0.823-0.115	472.0	57.21	529.84
60	40	5.51	0.675	1.58	696.4	0.862-0.313	250.0	46.29	440.75
40	60	8.81	0.911	1.56	669.22	0.856-0.284	272.1	47.61	428.98
20	80	12.89	1.311	1.60	644.3	0.852-0.260	291.9	48.74	402.68
0	100	17.565	1.982	1.62	643.03	0.848-0.240	309.86	49.72	396.93

R_Y = 3.437Å, R_Q = 2.840Å, τ =1.11 ns with [*Q*]. This might be attributed to static quenching of solute molecule in the vicinity of [*Q*] and transient effects arising from an initial time dependence of the concentration gradient or combination of them[36].

But if one assumes that only the first encounter is of interest in the case of efficient fluorescence quenching an initial average separation distance r_0 can be defined (sink radius) so that the diffusive region of interest for a first encounter is in the range $R \leq r \leq r_o$ such that all subsequent encounters are eliminated. This interpretation leads to the modification of Eq. (11) as:

$$\frac{1}{k_q} = \frac{1-(R/r_o)}{k_d} + \frac{1}{k_a} \quad \ldots (12)$$

This equation reduces to the reaction limited form ($k_q = k_a$) both for inefficient quenching ($k_a << k_d$) and for quenching in pure quenching solvents where $R = r_o$. In the diffusion controlled limit ($k_a >> k_d$) Eq. (12) reduces to:

$$k_q = \frac{k_d}{1 - R/r_o}$$

and k_q depends on the quenching concentration through r_o. Since, the sink radius (r_0) is identified with the most probable nearest neighbour initial separation, the appropriate distribution[28] requires that $r_o = (2\pi\, N'[Q]^{-1/3})$. Replacing r_o in Eq. (12) by $(2\pi\, N'[Q]^{-1/3})$ and k_d by its value, (i.e., $4\pi\, N'RD$) and dividing everywhere by the fluorescence life time of solute in the absence of quencher (τ) one obtains the modified S-V relationship[36] as:

$$K_{SV}^{-1} = (K_{SV}^{O})^{-1} - \frac{(2\pi N')^{1/3}}{4\pi N' D\tau}[Q]^{1/3} \quad \ldots (13)$$

Where, $K_{SV}^{O} = \dfrac{4\pi N' DR\, \tau\, k_a}{4\pi N' DR + k_a}$ a plot of K_{SV}^{-1} against $[Q]^{1/3}$ becomes linear with negative slope. Mutual diffusion coefficient *D* becomes directly accessible from the slope of the graph exemplified in Eq. (13) and K_{SV}^{O} is obtained at [Q] = 0 regardless of the relative magnitudes of k_a and $k_d\,(= 4\pi\, N'RD)$, whether quenching is diffusion limited or not. K_{SV}^{O} can also be written as:

$$K_{SV}^{O} = 4\pi\, N' DR'\, \tau \quad \ldots (14)$$

Where, *R'* is the distance parameter and has the same meaning as in the long time SCK model[36, 40] and is given as:

$$R' = R\,[1 + 4\pi\, N' DR / k_a]^{-1} \quad \ldots (15)$$

Then according to the theory discussed above if k_a is greater than k_d, (i.e., Eq. (11)) then the reactions are said to be diffusion limited[36], (i.e., for *R'*<*R*). But for *R`*>*R*, the bimolecular fluorescence quenching reactions are said to be diffusion limited[40] if the values of k_q determined from Eq. (12) are greater than $4\pi\, N' R' D$.

Therefore, according to Eq. (13) we need to determine the values of K_{SV}^{-1} and $[Q]^{1/3}$. Where, $K_{SV} = [I_O / I - 1]/[Q]$ and [*Q*] the quencher concentration from 0.000 to 0.100 M. For efficient quenching processes (concentration dependent) the value K_{SV} is often observed to increase with [*Q*]. Hence the values of K_{SV} were determined at each quencher concentration in all the solvent mixtures and the values of K_{SV}^{-1} are also accordingly determined. Figure 8 shows the plots of K_{SV}^{-1} against $[Q]^{1/3}$. From this figure we see that all the plots in TL-BL solvent mixtures are almost linear and small deviation may be due to experimental uncertainties. Hence, the linear dependence of K_{SV}^{-1} on the one-third power of quencher concentration [$Q^{1/3}$] within the error limits is confirmed[36]. Then the values of K_{SV}^{O} (i.e., S-V constant at [*Q*] = 0) and mutual diffusion coefficient *D* were obtained from the intercept and slope of the plot of K_{SV}^{-1} against $[Q]^{1/3}$, respectively. Using the values of K_{SV}^{O} and *D*, the distance parameter *R'* was determined from Eq. (16) and is given in Table 3 for all the solvent mixtures. It has been observed from Table 3 that R’>*R* in all the TL-BL mixtures and hence, the values of k_a cannot be determined. According to Joshi *et al.*[30] the bimolecular quenching reactions are said to be diffusion limited if the values of k_q are greater than $4\pi N'R'D$. Hence, the values of $4\pi N'R'D$ are calculated using the experimentally determined values of *R’* and *D* and both are given in Table 3. We see from Table 3, the values of k_q are greater than $4\pi N'R'D$, which is an expected result for diffusion limited reaction[40]. Further, we observe from Fig. 9 that the values of K_{SV} decreases as the viscosity of the solvent mixture increases. The high value of K_{SV} in polar solvent 1-butanol compared to non-polar solvent toluene may also be explained by the greater charge transfer character of the excited complex in the polar solvent. Figure 10 shows that the value of K_{SV} decreases as the dielectric constant of the solvent mixture increases. This effect of dielectric constant as function of K_{SV} suggests that the reacting species are of opposite charge. Here with reducing polar solvent percentage in the medium, dielectric constant decreases which in turn destabilizes the re-acting species and improves the reactivity by affecting the life time indicating increase in the rate of the reaction[16]. Observation of inverse dependence of viscosity in the studied sample predicts quenching to be purely controlled by material diffusion.

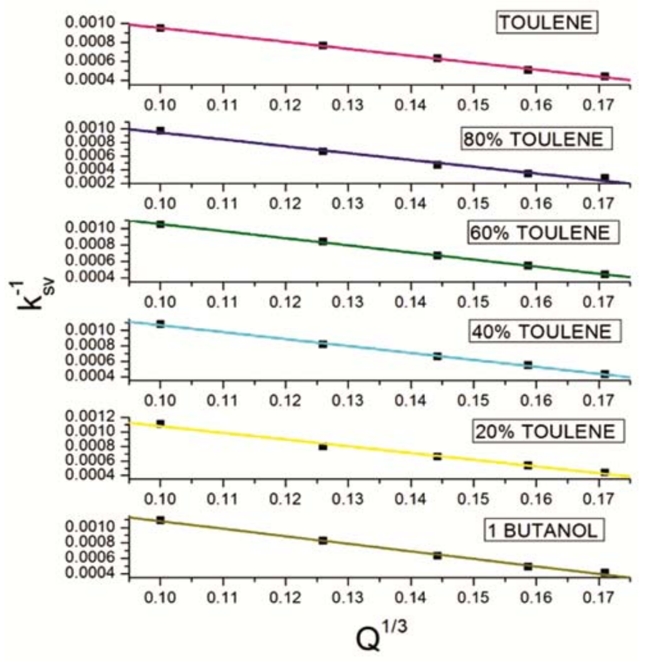

Fig. 8 — Plots of K_{sv}^{-1} versus $[Q]^{1/3}$for boronic acid dye+aniline system in different mixtures of toluene (TL) + 1butanol (BL) solvents: (i) 100 % TL + 0 % BL (ii) 80 % TL+ 20 % BL (iii) 60 % TL + 40 % BL (iv) 40 % TL + 60 % BL (v) 20 % TL + 80 % BL and vi) 0 % TL + 100 % BL.

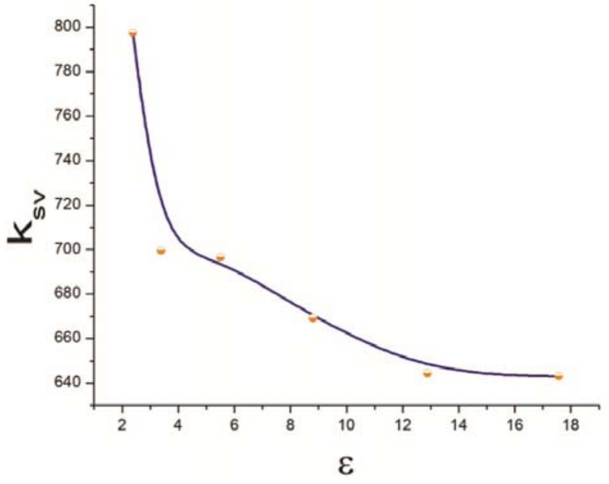

Fig. 9 — Variation of K_{sv} as a function of dielectric constant ε of dye.

Table 3 — Values of fluorescent life time (τ_0), K_{sv} (steady state quenching constant at [Q]= 0), mutual diffusion coefficient (D), distance parameter (R'), $4\pi N'DR'$ in solvent mixtures of toluene (TL) + 1butanol (BL) of different concentration in boronic acid dye at room temperature.

Solvent mixtures		τ_0 (ns)	K^0_{SV} (M^{-1})	$D \times 10^5$ ($Cm^{-2}s^{-1}$)	R' (A^0)	$4\pi N'DR' \times 10^{-9}$ ($M^{-1}s^{-1}$)
TL	BL					
100	0	1.11	595.23	25.35	27.97	536.24
80	20	1.32	515.46	15.70	32.89	390.50
60	40	1.58	520.83	15.09	28.89	329.63
40	60	1.56	507.61	14.62	29.43	325.39
20	80	1.60	497.51	13.86	29.67	310.94
0	100	1.62	485.43	12.97	30.55	299.64

$R (= R_Y + R_Q) = 6.277$Å

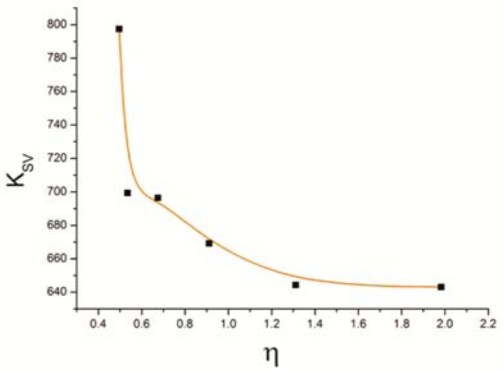

Fig. 10 — Variation of K_{sv} as a function of viscosityη of dye.

4 Conclusions

From the above discussion, we observe in dye that (i) 2 MEFPBA is preferential solvated by TL in its ground state and by more polar solvent in its excited state where dielectric enrichment is in role for preferential solvation in the excited state, (ii) the S-V plots show positive deviation, indicating efficient fluorescence quenching, (iii) the value k_q is greater than $4\pi N'R'D$ then bimolecular quenching reactions are said to be diffusion limited, (iv) the value of K_{SV} decreases with increase in viscosity shows quenching to be purely controlled by material diffusion, (v) the value of K_{SV} decreases with increase in dielectric constant of the solvent mixture suggesting reaction of opposite charge species and (vi) finite sink approximation model helps to recover R' and D directly from the plots K_{SV}^{-1} versus $[Q]^{1/3}$. In view of the above facts we conclude that quenching reaction is diffusion limited and both static and dynamic quenching processes are playing a role in this system.

References

1 Reichardt C & Welton T, *Solvents and solvent effects in organic chemistry*, John Wiley & Sons, NewYork, 2011.
2 Murthy S S, *Cryobiology*, 36 (1998) 84.
3 Snyder L R, *Rev Anal Chem*, 46 (1974) 1384.
4 Roy S & Bagchi B, *J Chem Phys*, 139 (2013) 034308.
5 Marcus Y, *Pharm Anal Acta*, 8 (2017) 537.
6 Wu S, Wang L, Zhang P, El-Shall H, Moudgil B, Huang X, Zhao L, Zhang L & Feng Z, *Hydrometallurgy*, 175 (2018) 109.
7 Fayed T & Etaiw S E, *Spectrochim Acta A*, 54 (1998) 1909.
8 Maitra A & Bagchi S, *J Molecular Liquids*, 137 (2008) 131.
9 Rothatgi-Mukherjee K K, *Fundamental of photochemistry*, Willey Eastern, New Delhi, 1986.
10 Lakowicz J R, *Principles of fluorescence spectroscopy*, Springer, Boston, MA, (1983) 257.
11 Tanielian C, Golder L & Wolff C, *J Photochem*, 25 (1984) 117.
12 Melavanki R M, Kusanur R A, Kadadevaramath J S & Kulkarni M V, *J Fluoresc*, 20 (2010) 1175.
13 Ding L, Liu H, Zhang L, Li L & Yu J, *Sens Actuators B: Chem*, 254 (2018) 370.
14 Koppal V V, Melavanki R M, Kusanur R A, Bhavya P & Patil N R, *J Molecular Liquids*, 260 (2018) 221.
15 Htun T, *J Fluoresc*, 14 (2004) 217.
16 Bhavya P, Melavanki R, Kusanur R, Sharma K, Muttannavar V T & Naik L R, *Luminescence*, (2018)1.Wiley online library.com/journal/bio.
17 Naik A B, Naik L R, Kadadevarmath J S, Pal H & Rao V J, *J Photochem Photobiol A: Chem*, 214 (2010) 145.
18 Bhavya P, Melavanki R M, Nagaraja D, Geethanjali H S, Kusanur R A & Manjunatha M N, *Can J Phys*, 94 (2016) 1384.
19 Molander G A, Trice S L & Dreher S D, *J Am Chem Soc*, 24 (2010) 17701.
20 Puchalski M M, Morra M J & Wandruszka R V, *Fresenius' J Anal Chem*, 340 (1991) 341.
21 Marcus Y, *Aust J Chem*, 36 (1983) 1719.
22 Suppan P, *J Chem Soc*, 83 (1987) 495.
23 Lerf C & Suppan P, *J Chem Soc*, 88 (1992) 963.
24 Laha A K, *J Chem Soc*, 88 (1992) 1675.
25 Roses M, Ortega J & Bosch E, *J Solution Chem*, 24 (1995) 51.
26 Skwierczynski R D & Connors K A, *J Chem Soc*, 2 (1994) 467.
27 Khajehpour M, Welch C M, Kleiner K A & Kauffman J F, *J Phys Chem A*, 105 (2001) 5372.
28 Kaur H, Koley S & Ghosh S, *J Phys Chem B*, 118 (2014) 7577.
29 Koley S, Kaur H & Ghosh S, *Phys Chem Chem Phys*, 16 (2014) 22352.
30 Khajehpour M & Kauffman J F, *J Phys Chem A*, 104 (2000) 7151.
31 Birks J B & Conte J C, *Proc R Soc A*, 303 (1968) 85.
32 Birks J B, Salate S C P & Leite M, *J Phys B*, 3 (1970) 417.
33 Samanta A, Richard W E, *J Phys Chem A*, 104 (2000) 8972.
34 Edward J T, *Chem Indus*, 1 (1956) 774.
35 Andre J C, Niclause M & Ware W R, *Chem Phys*, 28 (1978) 371.
36 Zeng H & Durocher G, *J Lumin*, 63 (1995) 75.
37 Keizer J, *J Phys Chem*, 86 (1982) 5052.
38 Keizer J, *J Chem Soc*, 105 (1983) 1494.
39 Keizer J, *J Am Chem Soc*, 107 (1985) 5319.
40 Joshi G C, Bhatnagar R, Doraiswamy S & Periasamy N N, *J Phys Chem*, 94 (1990) 2908.